
Article:
Patton, H., Swift, D.A., Clark, C.D. et al. (3 more authors) (2015) Automated mapping of glacial overdeepenings beneath contemporary ice sheets: Approaches and potential applications. Geomorphology, 232. 209 - 223. ISSN 0169-555X

https://doi.org/10.1016/j.geomorph.2015.01.003

Automated mapping of glacial overdeepenings beneath contemporary ice sheets: approaches and potential applications

Henry Patton[a,b,1,†], Darrel A. Swift[a,*,†], Chris D. Clark[a], Stephen J. Livingstone[a], Simon J. Cook[c], Alun Hubbard[b]

[a]*Department of Geography, University of Sheffield, Winter Street, Sheffield, S10 2TN, UK*

[b]*Department of Geology, University of Tromsø – The Arctic University of Norway, N-9037 Tromsø, Norway*

[c]*School of Science and the Environment, Manchester Metropolitan University, Chester Street, Manchester, M1 5GD, UK*

[1]*Present address: Department of Geology, University of Tromsø – The Arctic University of Norway, N-9037 Tromsø, Norway*

[*]*Corresponding author. Email d.a.swift@sheffield.ac.uk. Telephone +44 114 222 7959.*

[†]*These authors contributed equally to this work.*

Abstract Awareness is growing of the significance of overdeepenings in ice sheet systems. However, a complete understanding of overdeepening formation is lacking, meaning observations of overdeepening location and morphometry are urgently required to motivate process understanding. Subject to the development of appropriate mapping approaches, high resolution subglacial topography data sets covering the whole of Antarctica and Greenland offer significant potential to acquire such observations and to relate overdeepening characteristics to ice sheet parameters. We explore a possible method for mapping overdeepenings beneath the Antarctic and Greenland ice sheets and illustrate a potential application of this approach by testing a possible relationship between overdeepening elongation ratio and ice sheet flow velocity. We find that hydrological and terrain filtering approaches are unsuited to mapping overdeepenings and develop a novel rule-based GIS methodology that delineates overdeepening perimeters by analysis of closed-contour properties. We then develop GIS procedures that provide information on overdeepening morphology and topographic context. Limitations in the accuracy and resolution of bed-topography data sets mean application to glaciological problems requires consideration of quality-control criteria to (a) remove potentially spurious depressions and (b) reduce uncertainties that arise from the inclusion of depressions of nonglacial origin, or those in regions where empirical data are sparse. To address the problem of overdeepening elongation, potential quality control criteria are introduced; and discussion of this example serves to highlight the limitations that mapping approaches — and applications of such

approaches — must confront. We predict that improvements in bed-data quality will reduce the need for quality control procedures and facilitate increasingly robust insights from empirical data.

Keywords: overdeepenings; automated landform mapping; glacial erosion; landscape evolution; Antarctica; Greenland

1. Introduction

The mechanisms by which glaciers and ice sheets form spectacular alpine and fjord landscapes are well known, and such landscapes have been exploited widely for purposes of palaeoglaciology and process understanding (e.g., Glasser and Bennett, 2004). Recently, this understanding has been aided by implementation of simple ice-erosion laws within numerical models, which are able to simulate patterns of glacial incision with compelling success (e.g., Harbor, 1992; MacGregor et al., 2000; Kessler et al., 2008). However, the mechanisms that produce overdeepenings (Fig. 1) remain unclear, and the implementation of candidate processes within ice-erosion models has met with limited success (e.g., Egholm et al., 2012). An important constraint on the development of process understanding is the absence of quantitative studies that have characterised overdeepening distribution and morphology. This contrasts sharply with the advances that have taken place with regards to the understanding of other subglacial phenomena, such as drumlins (e.g., Clark et al., 2009). In particular, improvements in remote sensing mean these studies have provided robust morphological data that has motivated development and testing numerical models that simulate ice sheet and landscape evolution processes (e.g., Fowler, 2009, 2010; Fowler et al., in press).

Cook and Swift (2012) have argued that the glaciological significance of the reverse-bed gradient that occurs in the presence of an overdeepening (Fig. 1C) is such that a complete understanding of overdeepening formation and morphology is essential to elucidate and understand critical ice-bed processes and to inform predictions of past and present ice-mass behaviour. First, empirical (e.g., Iverson et al., 1995) and theoretical work (e.g., Röthlisberger and Lang, 1987; Creyts and Clarke, 2010) demonstrates that overdeepenings raise subglacial water pressures by reducing drainage system transmissivity, thus affecting ice-bed coupling and basal sliding. Second, the amplitude and wavelength of topography at the ice sheet bed is of fundamental significance to ice sheet sliding laws (Schoof, 2005); and third, marine outlet systems that terminate on adverse slopes are vulnerable to rapid 'collapse' (Schoof, 2007; Nick et al., 2009). Further, the processes of overdeepening evolution are poorly understood. Cook and Swift (2012) proposed that patterns of subglacial erosion and deposition, which are dictated by the ice surface gradient (cf. Hooke, 1991; Alley et al., 2003), mean all glacier and ice sheet beds should tend toward a uniformly overdeepened long-profile, with deepest

erosion near the long-term average equilibrium line altitude (ELA) (e.g., Boulton, 1996; Hallet et al., 1996; Anderson et al., 2006). However, other observations indicate that ice-water-sediment-erosion (IWSE) feedbacks produce very localised, deep glacial erosion (e.g., Hooke, 1991; Alley et al., 2003) and may therefore act as an important constraint on overdeepening size and morphology (Cook and Swift, 2012).

The increasing availability of high-resolution subglacial topography data sets for the extant ice sheets (e.g., Bamber et al., 2013; Fretwell et al., 2013) indicates potential now exists to achieve major advances. For example, the ability to relate morphological characteristics to ice sheet parameters means that expectations of overdeepening influence on ice dynamics are eminently testable. Further, parameterisation of IWSE processes in numerical ice-erosion models that couple the flow of ice, water, and sediment (e.g., Egholm et al., 2012) — and increasingly sophisticated treatments of the ice flow (Egholm et al., 2011), erosion (e.g., Iverson, 2012), and water flow (e.g., Werder et al., 2013) — will benefit from quantitative data on overdeepening location and morphology that facilitates evaluation of model-based landscape evolution simulations. We therefore develop a computationally efficient GIS-based method for mapping overdeepenings, and, in anticipation of the data that may be required to test empirical relationships and model-based outputs, we develop additional methods that enable characterisation of overdeepening shape, including long- and cross-profiles that pass through the deepest point. These methods require delimitation of the overdeepening perimeter and identification of in- and outflow points, and also require identification of overdeepenings within overdeepenings (i.e., nested overdeepenings; Fig. 1D). From these phenomena, further metrics — including elongation ratio (cf. Clark et al., 2009), normal and adverse slope lengths and gradients, and planform area — can then be derived (Fig. 2).

To illustrate a possible application of our method, we seek to evaluate a probable relationship between overdeepening elongation ratio and ice velocity using subglacial topography data sets and ice surface velocity data for the Antarctic and Greenland ice sheets. Such applications are limited by the quality of the metrics that present data sets permit, and we use this example to motivate (i) the development of quality control criteria appropriate to current data set uncertainties and (ii) a discussion of the sources of uncertainty that affect the proposed relationship. Whilst traditional methods of geomorphological mapping at this scale are inappropriate, we find that automated mapping approaches and their applications also have limitations. Importantly, such approaches need to be undertaken with careful appreciation of data set quality and resolution, the probable presence of features of nonglacial origin, and the different timescales of ice mass and landscape response.

2. Study areas and data sets

2.1. Study areas

The landscape beneath present-day ice sheets provides an unparalleled opportunity to elucidate ice-bed processes and evolution because of the size of the ice-covered area and the absence of thick post-glacial deposits that in palaeoglaciated landscapes accumulate within areas of deep erosion. Comprehensive subglacial topography data sets for the Antarctic (Bedmap2) and Greenland ice sheets have recently been made available (Bamber et al., 2013; Fretwell et al., 2013), and these are used in the example application of our methods in section 5. For practical purposes, the development of these methods was undertaken on a relatively small domain surrounding the Byrd Glacier catchment and Transantarctic Mountains, adjacent to the Ross Ice Shelf, in East Antarctica (Fig. 3). This 5.22 x 10^5 km^2 region provides an excellent methodological test-bed, combining substantial variability in relief with the presence of a large number of bed depressions that exhibit a range of depths and areas.

2.2. Antarctic subglacial topography

The Bedmap2 data set provides subglacial and continental shelf topography for the Antarctic continent (Fretwell et al., 2013) using the most up-to-date compilation of empirical ice thickness measurements for the Antarctic ice sheets. Raw ice thickness data for Bedmap2 have been derived from a variety of sources, including direct airborne radar sounding and seismic measurements; satellite altimetry and free-air gravity surveys; and 'synthetic' data computed using a 'thin-ice' model. The rationale for including modelled topography within the source data was to prevent rock outcrops from overly skewing the ice thickness distribution in mountainous areas where few empirical measurements exist. Although this output gives the appearance of accurate relief within ice-marginal mountain ranges, this topography, notably, is not directly constrained by any empirical data. Continental shelf topography is derived from the GEBCO 2008 bathymetric compilation mosaiced with sub-ice shelf data from Timmermann et al. (2010).

The Bedmap2 topography is rendered on a 1-km grid, but empirical and synthetic measurements of ice thickness were sampled at 5 km, primarily because the distribution of empirical measurements (which require interpolation (kriging) to form a continuous surface) did not warrant a higher resolution (Fretwell et al., 2013). Notably, the spatially nonuniform distribution of ice thickness measurements obtained by airborne radar surveys (in which across-track sampling density is potentially 3 or 4 orders of magnitude lower than the density along the flight tracks) means that even large, valley-scale features may be absent or resolved poorly. Furthermore, the fragmentary nature of completed radar surveys carried out across Antarctica has left many regions sparsely constrained. For example, in Bedmap2, 80% of grid cells have data within 20 km; and the greatest distance from a grid cell to the

nearest data point (the 'poles of ignorance') is ~ 230 km (Fretwell et al., 2013). For this reason, the nongenetic term *depression* is used in the methodological sections of this study, thereby avoiding the implication that all basin-like features in digital elevation model (DEM) surfaces are genuine closed-depressions and/or glacial overdeepenings.

2.3. Greenland subglacial topography

Subglacial and continental shelf topography for Greenland is provided by Bamber et al. (2013). As with Bedmap2, topography in this data set is rendered on a 1-km grid with subglacial topography mainly derived using ice thickness measurements obtained from airborne radar surveys and satellite observations. As such, similar error sources, assumptions, and levels of uncertainty exist. Continental shelf topography is sourced from the most recent IBCAO (International Bathymetric Chart of the Arctic Ocean) compilation of offshore bathymetric data sets (Jakobsson et al., 2012), supplemented with additional soundings from Jakobshavn fjord. Notably, where bathymetry is not well known, or observations do not exist, bed elevations are often underestimated by up to several hundred metres, particularly within fjords (Bamber et al., 2013).

2.4. Additional data sets

Higher-resolution ice thickness data sets for several areas of Antarctica were obtained from the Centre for Remote Sensing of Ice Sheets archive (CReSIS; https://data.cresis.ku.edu) to evaluate the implications of DEM resolution for the delineation of overdeepening perimeters. These products, which have restricted geographical coverage, are derived from airborne radar surveys and are published at a grid spacing of 500 m. Ice-surface velocity data derived from InSAR observations over Antarctica and Greenland were sourced from data sets compiled by Rignot et al. (2011a) and Joughin et al. (2010a), respectively.

3. Automated mapping of overdeepenings

3.1. Delimitation of overdeepenings in the landscape

A key challenge in mapping geomorphological phenomena is delineating their boundaries. For example, overdeepenings do not represent isolated pockets of deep glacial erosion in an otherwise unmodified fluvial landscape. Most frequently, overdeepenings occur as areas of deeper erosion in the floors of deep, glacially carved valleys (cf. Cook and Swift, 2012) and, as such, the flanks of an overdeepened basin are inseparable from those of the host valley. The use of hydrological tools to delineate overdeepenings (see section 3.2.1) by means of 'filling sinks' does not therefore necessarily have a strong, physical basis. Further, subaerial and subglacial hydraulic gradients will differ, meaning

that an overdeepening that in the subaerial environment contains a lake will only contain a subglacial lake if the gradient of the adverse bedslope exceeds 11 times that of the ice-surface gradient (the 'ponding' threshold; Clarke, 2005) (Fig. 1C). The ‘surface’ of such a lake will be inclined in the opposite direction to ice flow, and the gradient of the surface will vary in response to changes in ice-surface gradient during glacial advance and retreat.

To avoid consideration of such complexities, we follow the definition provided by Cook and Swift (2012), who use *overdeepening* (verb) to describe the excavation of a topographic depression that, subglacially, would require ice, water, and sediment to traverse a locally reversed (or adverse) slope. This usage therefore describes the creation of a specific landform, an *overdeepening* (noun), which on deglaciation would form a sedimentary basin or lake (cf. Fountain and Walder, 1998). This definition of an overdeepening as a subaerial ‘closed depression’ means that the elevation at the outflow point can be used to delineate the perimeter. Mapping of closed depressions in predicted subglacial hydraulic potentials (cf. Shreve, 1972) is avoided intentionally because depression form and location would depend partly on the morphology of the ice surface, which is inherently variable. A classification based on purely morphological grounds is therefore independent of glaciological processes. Clearly, closed depressions can also be formed by nonglacial processes, including tectonic processes (e.g., by faulting), whilst some mapped depressions are artefacts resulting from interpolation between sparse empirical data. Methods of identifying erroneous depressions and tectonic basins are also therefore considered in this study.

Despite the morphological simplicity of closed depressions, mapping methodology must overcome several important challenges. Firstly, automated analyses of DEMs at the ice sheet scale, even at 1-km resolution, require computationally efficient techniques. Secondly, like other bedforms (cf. Clark et al., 2009), overdeepenings tend to develop a distinctive ovoid planform (Cook and Swift, 2012), but constraints imposed by topography often produce sinuous overdeepenings that follow the axes of large troughs (e.g., Fig. 1B), while others are influenced by geological structures or changing phases of ice flow direction, resulting in circular or irregular shapes. Thirdly, overdeepenings are frequently nested (e.g., Fig. 1D), with larger examples occasionally containing many generations of nesting. Finally, many overdeepenings beneath contemporary ice sheets may be relict landforms that represent erosion during earlier stages of glaciation, which may limit meaningful analysis of mapping results. For example, ice flow direction during depression formation, and thus the location of in- and outflow points, cannot always be established.

3.2. Delineation methods

Three GIS-based methodologies were evaluated for the purpose of delineating depressions in a DEM surface that would constitute subaerial closed-depressions in a landscape. The third approach was adopted for this study.

3.2.1. Hydrological filling

In the post-glacial landscape, overdeepenings are sinks for water and sediment (e.g., van Rensbergen et al., 1999; Preusser et al., 2010). An instinctual approach to mapping overdeepenings is therefore to use GIS hydrological tools to identify sinks (or areas of internal drainage) across the digital terrain (e.g., Arnold, 2010). 'Fill' tools offer the simplest approach and work by filling sinks to capacity, thereby creating a 'depressionless' DEM. A major disadvantage of this method is that smaller depressions located within larger depressions cannot be delimited, meaning overdeepenings within tectonic basins or rifts, or smaller overdeepenings nested within larger overdeepenings, are not mapped (Fig. 3A). The wide size range exhibited by overdeepenings (Cook and Swift, 2012) means those solutions to this problem that use fill criteria to limit the size of the fill area for individual depressions are unworkable at the scale of whole ice sheets.

3.2.2. Terrain filtering

A more sophisticated yet computationally simple approach to mapping overdeepenings is to apply signal-processing techniques to the DEM surface (e.g., Leonowicz et al., 2009; Stumpf et al., 2013). This approach considers the landscape as a three-dimensional waveform within which depressions and mountain peaks represent anomalous interference. By filtering the elevation data at specific wavelengths, a smoothed surface largely voided of relief (interference) can be created. Overdeepened topography can then be extracted by calculating the negative residuals beyond a given threshold compared to its original form. Figure 3B shows how a two-dimensional, circular (200 km), low-pass Gaussian filter of the form

$$f(x,y)=(1/2\pi\sigma^2)e^{-[(x-\mu_x)^2+(y-\mu_y)^2]/(2\sigma^2)} \quad (1)$$

where sigma (σ) and mu (μ) are the standard deviation and mean of the elevation distribution, respectively, can be used to produce a map of probable areas of overdeepening. In contrast to basin extents mapped using hydrological filling techniques (above), this approach lacks precise thresholds required for delimiting closed depression perimeters. Furthermore, the approach does not enable mapping of nested features. A more rigorous GIS-based approach is therefore needed that is appropriate to the complex morphology of large depressions.

3.2.3. Contour tracking

A final approach to delineating overdeepenings is to track changes in closed-contour length as an observer moves away from an elevation minimum. The novel contour-tracking process developed for this study is threefold. Firstly, a terrain analysis mask is calculated that delimits depression-like areas in the DEM surface (Figs. 4A–B). By eliminating large areas of the surface that are not depression-like, this initial step greatly enhances computational efficiency at the ice sheet scale. Secondly, locations of elevation minima are pinpointed using zonal statistical analyses to find the minimum point within each closed-contour that intersected the terrain-analysis mask (Fig. 4C). Finally, changes in contour length are tracked away from each elevation minima to identify sharp increases in length that would indicate the breach of a closed depression (Figs. 5A-B). The steps detailed below were implemented using toolboxes and commands found within ArcGIS 10.1 and GRASS GIS, with automated workflow achieved using packages within Python such as ArcPy.

Step 1 – Terrain analysis mask. Many existing methods of automated terrain analyses have their roots in differential geometry, using combinations of morphometric parameters such as slope, gradient, curvature and aspect to classify the form of the DEM surface (e.g., Evans, 1980; Wood, 1996; MacMillan et al., 2000; Wilson and Gallant, 2000; Drăguţ and Blaschke, 2006; Klingseisen et al., 2008; Brenning, 2009; Saha et al., 2011). Here, two parameters are used to delimit broad areas of depression-like relief: plan curvature (horizontal curvature, intersecting with the *XY* plane) and minimum curvature in the direction perpendicular to the direction of maximum curvature. The quantitative foundation to this methodology thus creates several user-specified parameters that can be adjusted depending on the desired mapping goals (cf. Table 1). For example, plan curvature and minimum curvature can be tuned to mask only small cirque-like features that are confined by high topography.

Step 2 – Finding elevation minima. Elevation minima are found by running a zonal statistical tool on the depression-like areas identified in step 1. Where contours are completely within the terrain analysis mask, a grid of points with elevation attributes is created, from which points of minimum elevation associated with each contour are deduced. Repeat points, or erroneous elevation peaks, can be removed by systematic comparison with the elevation and the ID of the bounding contour.

Step 3 – Contour analysis. Depression perimeters are delineated by determining the highest elevation 'bounding contour' using a process of 'contour-tracking'. This method works by measuring the change in contour length between successive contours at increasing distance from the point of elevation minima (Fig. 5A). In the case of depressions, contour lengths will increase in size, and contour length will increase rapidly when a depression is 'breached'. For this study, a change in contour length of

90% from the preceding contour was chosen, which represents a factor-of-three increase in the bounded area. This method was used to identify generations of nested depressions (Fig. 5B) by running multiple passes whilst 'ignoring' previously identified depression breaches.

A range of parameters can be specified during this process (Table 1). For this study, values were chosen that provide sensible results, but these are far from definitive. In addition, classification of nested depressions can be undertaken, and for this study a simple top-down approach based on nested depression order was applied (Fig. 5C).

4. Automated extraction of overdeepening metrics

Whilst mapping methods (above) can provide qualitative information on the distribution, planform morphology, and nesting of probable overdeepenings, further methods are required to extract information on overdeepening form (e.g., Fig. 2). The GIS-based methods suitable for extracting such metrics from very large numbers of mapped overdeepenings are described below.

4.1. Depression in- and outflow points

The identification of depression entry and exit points is a critical step in the measurement of depression length, elongation, and the morphology of normal and adverse slopes. In order to provide adaptability to different contexts, three approaches are presented here. The first two are topographic and hydrological methods that utilise the bed topography alone and may be appropriate where ice thickness data are not available (e.g., in palaeo domains), although we also consider a more sophisticated hydrology-based approach that makes use of ice thickness data to infer subglacial water flow directions. The third uses only simple analysis of ice-surface elevations above the depression perimeter. All three approaches have methodological limitations, a summary of which is given in Table 2. Although methods that infer subglacial water flow may offer advantages for understanding some processes (see below), the ice-surface–based approach was considered to be the most robust (see Discussion).

4.1.1. Topography based

Where grounded ice thickness data do not exist (e.g., continental shelves and palaeo ice sheet domains), in- and outflow points can be inferred by identifying broad trends in landscape elevation by means similar to the filtering method presented above (Section 3.2.2). However, thick ice sheets may become independent of topography and may subsume and dissect mountain ranges, meaning ice flow directions can reverse as ice sheets grow. For the Byrd test domain, a 1500 km^2 moving window is required to overcome the influence of the Transantarctic Mountains and identify a general trend in

relief that reflects the westward flow of the East Antarctic Ice Sheet. By reducing the size of this moving window, more localised trends in elevation change can be extracted, which may be suitable for defining in- and outflow points during periods when glaciation was more restricted and smaller ice masses occupied only higher elevations. However, different sectors of a single ice sheet can be characterised by contrasting styles of glaciation, meaning this method can be difficult to apply across ice sheet scale domains.

4.1.2. Hydrology based

An intuitive approach to identifying in- and outflow points where ice thickness data are absent is to use 'hydrological tools' to calculate water flow direction and flow accumulation rasters for the DEM surface. Because ice flow in areas of deep erosion and overdeepening development is directed by topography, flow routing can be used to infer locations where maximum ice flux enters and leaves each depression. However, the assumption that subaerial water flow represents an accurate proxy for ice flow does not, as discussed above, hold true for ice sheets that subsume mountainous landscapes. If ice thickness is known, a more direct approach can be used (see 4.1.3 below), but the availability of ice thickness data presents a further hydrology-based approach, which is to infer subglacial water flow direction through calculation of hydraulic potentials (cf. Shreve, 1972) at the ice-bed interface (e.g., Livingstone et al., 2013). This method is likely to provide a better approximation of the pathways of water and sediment through an overdeepening than ice-flow–based methods and may therefore be useful for understanding certain overdeepening-related processes and feedbacks. However, flow patterns are sensitive to changes in ice-surface geometry and will not follow the deepest path through an overdeepening where the adverse slope approaches or exceeds the ponding threshold (Clarke, 2005), meaning the identification of outflow points using this method is unlikely to be robust.

4.1.3. Ice-surface based

The preferred method for identifying in- and outflow points in this study uses the elevation of the overlying ice sheet surface. Assuming that the surface of ice flowing immediately above an overdeepening approximates a uniform plane that slopes in the direction of flow, the points of maximum and minimum ice-surface elevation that lie above the bounding contour of the depression (Fig. 6) will provide a reasonable approximation for the principal entry and exit points in terms of the greatest flux of ice. Where multiple points of equal ice-surface elevation exist around the depression edge, a single in- or outflow point can be determined by choosing the point most distant from the basin minima. Given the size of depression that can be mapped from a 1-km resolution DEM, the ice-surface elevation data set is sufficiently precise to enable the identification of in- and outflow points even for depressions in the centre of an ice sheet, and application to the test area domain demonstrates that this method is robust in most contexts (Fig. 7). The suitability of this method will, however, collapse under

flat ice surfaces, such as those of ice shelves or above large subglacial lakes, and where overdeepening planform is highly complex.

4.2. Depression morphology and context

Following the identification of depression minima, bounding contours, and in- and outflow points, a range of descriptive profiles and quantitative metrics can be extracted for each depression (e.g., Fig. 2). Many of the metrics are readily calculated using simple GIS techniques and to give a thorough description here would be unnecessary. However, some, such as the long-profile and the calculation of elongation ratio for sinuous or asymmetric depressions, require bespoke methods.

4.2.1. Long-profiles

For depressions with sinuous planforms, the path of a long-profile that follows the deepest route through the depression is far removed from a straight line that joins the in- and outflow points. A convenient solution is to calculate a 'least-cost' path between the in- and outflow points that passes through the depression minimum (Fig. 7B). The in- and outflow locations and position of the depression minimum can then be used to divide the profile into normal and adverse slopes. For adverse slopes with gradients that are below 11 times the ice-surface gradient (Clarke, 2005), this path will approximate the route taken by subglacial water through the depression, and as noted previously this may offer some advantages. However, steeper adverse slopes will cause flow to flow around the overdeepening or distribute across the adverse slope. Consequently, hydrological methods for determining the depression long-profile were deemed unsuitable.

4.2.2. Depression shape

The shape of each mapped feature can provide important information on its probable origin and history of erosion. For example, many glacigenic geomorphological phenomena demonstrate ovoid or elongate forms (see section 5.1), meaning ovoid depressions may be considered more likely to have a glacial origin than those with more complex planform morphologies, and a glacial origin may be considered even more secure for those with ovoid planforms that are elongate in the direction of ice flow. Small, isolated, and circular depressions appear to be characteristic of artefact depressions created by kriging at flightline intersections in regions of sparse empirical data, giving a 'pockmarked' appearance to the DEM surface.

Two shapes are thus of interest: circular and elongated (i.e., ovoid). Absence of elongation can be assessed using a minimum bounding geometry methodology, whereby a depression is enclosed within a polygon that is defined by its minimum possible area (Fig. 8A). Where a depression fills more than 60% of a square polygon, it can be classified as 'circular'. However, elongation cannot be assessed

using this method if a depression exhibits strong sinuosity (e.g., Fig. 1B) or a complex planform. As a result, we have developed a novel method for assessment of elongation in which elongation is determined with respect to the presumed direction of ice flow at all points along the depression long-profile. This was be achieved by calculating the mean width of the depression perpendicular to the least-cost transect at regular intervals along the long-profile (Fig. 8B). Further, the threshold for elongation was defined as an elongation ratio (transect length divided by mean width) that exceeds 2. Depressions that exhibit neither circularity nor elongation in the direction of ice flow are deemed 'unclassified'.

4.3. Contextual classification

Overdeepening form and location is likely to be influenced by a range of local factors that affect erosion potential, including lithological changes or weaknesses and the location of moulins that direct surface runoff to the glacier bed (Hooke, 1991; Herman et al., 2011; Cook and Swift, 2012). Often, the simplest method for isolating such external drivers will be by cross-referencing depression location and/or relevant metrics with other numerically modelled or empirical data sets. Other factors can be isolated by automated classification of mapped depressions using such data sets. For example, empirical observations have indicated that topographic-focussing of ice flux in regions of high relief is a strong control on overdeepening location and depth (e.g., Kessler et al., 2008; Roberts et al., 2010). In this instance, a depression can be classified as 'topographically confined' using a simple proximity-based GIS-method that calculates the mean elevation of the topography within a small (20 km) buffer of the depression perimeter.

5. An assessment of the influence of overriding ice velocity on overdeepening morphology

Application of the methods outlined above to bed-topography data sets for Antarctica and Greenland (Bamber et al., 2013; Fretwell et al., 2013; Patton et al., in prep) produces a database of > 13,000 bed depressions (including nested depressions). To demonstrate the potential insight that can be gained from such data sets, we test for a possible relationship between overriding ice velocity and overdeepening morphology. Acknowledging the important uncertainties associated with current subglacial topography data sets (see Discussion), we apply strict quality-control criteria to our mapping of bed depressions and analyses of their metrics.

5.1. Motivation

It has been proposed that many glacially moulded bedforms (including flutes, drumlins and mega-scale lineations) lie on a continuum of scale that reflects the velocity of overriding ice (e.g.,

Heidenreich, 1964; Stokes and Clark, 2002; Clark et al., 2009). The elongation ratio (ER) of these phenomena is assumed to correlate with ice velocity, meaning high ER values can be used to infer ice-streaming conditions (e.g., Clark, 1993; Stokes and Clark, 1999; King et al., 2009; Ó Cofaigh et al., 2013). A similar correlation may exist for overdeepenings because fast-flowing ice should enhance rates of headward erosion by quarrying and abrasion (cf. Hooke, 1991; Herman et al., 2011) and rates of sediment evacuation and abrasion at the overdeepening lip (cf. Alley et al., 2003). A demonstration of this relationship would have significant value for palaeoglaciological research because it would provide information on former ice velocities in regions where erosional processes have dominated or the preservation of depositional bedforms has been poor.

5.2. Quality-control procedures

Comparison of mapping results for Bedmap2 and for the higher-resolution CReSIS data set (Fig. 9) demonstrates that the spatially variable distribution of empirical measurements in both data sets produces artefacts that are mapped as bed depressions. In the Bedmap2 topography, these artefacts mainly constitute smaller, isolated, spherical depressions that are aligned with the flightlines used to collect airborne radar measurements of ice thickness (Fig. 9C). Mapping of the same domain from the higher-resolution data set identifies a significantly greater number of bed depressions, many of which have a similar isolated, spherical appearance, albeit at a smaller scale commensurate with the increased resolution of the data set and density of flightlines (Fig. 9D). In contrast, the first-order characteristics of larger depressions do not differ substantially when mapped using the higher-resolution data set, as demonstrated by planform (Fig. 9C–D) and long-profile (Fig. 9E) characteristics of the Byrd Glacier depression. Mapping from higher-resolution data sets therefore improves the detail of the outlines (and thus metrics) of larger and some smaller depressions, but artefact depressions are still present.

To avoid the inclusion of spurious metrics from artefact depressions, mapping of overdeepenings from gridded data sets requires application of quality control criteria regardless of data resolution. For this study, a suite of criteria have been considered and applied that are based on known data set uncertainties (cf. section 2.2):

(i) Bed-elevation uncertainty. Absolute bed-uncertainty data beneath grounded ice is provided with the DEMs for Greenland and Antarctica (Bamber et al, 2013; Fretwell, et al., 2013). Although this is a good measure for estimating uncertainties in overdeepening absolute depth (i.e., the elevation of the deepest point in relation to sea level), it is not a robust criterion for assessing adequate delineation of mapped features, which is dependent on relative uncertainties in the

immediate area of the bed. For this reason, criteria based on flightline density and depression size (below) were also considered.

(ii) Flightline density. Criteria were used to specify a minimum depression width in regions of sparse empirical data, resulting in the removal of small, isolated depressions characteristic of artefact depressions produced by kriging. Areas of sparse data were identified using a flightline density mask that showed the density of flightlines within a 10-km radius of each grid cell. Depressions with widths < 20 km were excluded if they did not intersect areas with densities > 0.11, which is roughly equivalent to two flightlines within the given radius. The choice of criteria reflects the observation by Fretwell et al. (2013) that absolute errors in elevation generally increase over distances of up to 20 km, beyond which errors appear largely uncorrelated with distance.

(iii) Depression size. Several size criteria were employed. Firstly, large features (e.g., tectonic basins) were removed by excluding depressions with bounding contours exceeding 2000 km in perimeter (an area equivalent to 1.5 times the catchment area of Pine Island Glacier, Antarctica; cf. (Vaughan et al., 2006). Depressions beyond this size are unlikely to have a glacial origin. Secondly, in regions with flightline densities > 0.11, depressions with adverse slopes shorter than 5 km were excluded because depressions of this size were unlikely to be adequately resolved by empirical measurements. Finally, a minimum overdeepening depth of 40 m was applied regardless of other criteria because shallow depressions are likely to have many sources, including kriging, bed elevation uncertainty, and geology. This value is intermediate between the minimum published absolute uncertainty values for the Bedmap2 (±66 m) and Greenland (±10 m) data sets (Bamber et al, 2013; Fretwell, et al., 2013).

(iv) Elongation with respect to the current ice flow direction (cf. section 4.2.2). In accordance with the majority of landforms sculpted by flowing ice (e.g., flutes, drumlins, roche moutonnées, troughs), overdeepenings are generally elongate in the direction of ice flow. This criterion can therefore be applied to exclude potentially nonglacial depressions. Though some genuine overdeepenings will be excluded, including those with complex planforms formed under previous ice flow configurations, strict filtering of landforms on the basis of ice flow direction will be beneficial for many applications because it should remove 'relict' landforms or those with complex morphologies that are unlikely to be in equilibrium with present ice sheet processes.

(v) Topographic confinement. Empirical observations indicate that overdeepenings are most common where ice flow is topographically confined (e.g., within valleys and outlet glacier troughs), meaning this criterion can be applied in conjunction with (iv) to exclude probable nonglacial depressions. Notably, by favouring depressions that are located within troughs where ice flow

direction is likely to have been stable over many glacial cycles, this criterion will exclude depressions with morphologies that may have evolved under varying ice flow configurations. For this study, depressions were classified as topographically confined if the mean elevation of topography surrounding the depression exceeded the elevation of the lip by a value > 500 m (cf. section 4.3; Fig. 8C).

5.3. Results and interpretation

To test the relationship between overdeepening ER and ice velocity for contemporary ice sheets, our mapping methods allow the ER of Greenland and Antarctic depressions to be plotted against ice-surface velocities (Joughin et al., 2010b; Rignot et al., 2011b) measured above the deepest point in each depression (Fig. 10). Because of uncertainties regarding the origin of nested depressions, we restrict our analysis to 'parent' depressions that are elongated in the direction of ice flow and that pass the other quality criteria detailed above. In addition, we separately analyse the subset of depressions that can be categorised as 'topographically confined'. Not unexpectedly, plots of ice velocity versus ER (Fig. 10) show substantial scatter, demonstrated by very low R^2 values, that is consistent with the limitations of the source data sets and the simplicity of our approach. Nevertheless, significance values for three of the plots are < 0.05 and therefore do not exclude a relationship. This leaves open the possibility that improvements in bed data quality, and quality control criteria, may provide a stronger foundation for such a link. Furthermore, significance values are strongest for topographically confined depressions, despite the number of depressions within these subsets being significantly smaller. This is particularly evident for Greenland, where the relationship for elongated depressions is not statistically significant. The application of strict quality criteria means that the inclusion of spurious depressions arising from DEM artefacts is not thought to be a significant influence on the observed relationships.

6. Discussion

6.1. Overdeepening identification and mapping approaches

A necessity for automated mapping approaches at the scale of whole ice sheets is the development of simple yet robust methods of landform delimitation (e.g., Saha et al., 2011). Overdeepenings present a considerable challenge in this respect because closed-depressions can arise from glacigenic and geological processes, though large tectonic basins (e.g., Wilkes subglacial basin) are easily excluded and smaller tectonic basins (e.g., the Vostok basin in East Antarctica) are relatively rare. An overriding concern, however, is how to define overdeepenings as mappable landforms (see Section 3.1). In particular, because the movement of ice, water, and sediment at the ice sheet bed is driven by the ice sheet gradient, our approach may not be suited to applications that aim to understand the

influence of overdeepenings on specific glaciological processes. For purposes of understanding the formation of features that evolve over time periods that span many glacial cycles, these processes do not suggest suitable mapping criteria. We therefore delimit overdeepenings as 'subaerial' closed-depressions (e.g., Fountain and Walder, 1998) and have found this method to be effective and robust at the ice sheet scale.

The time scale of overdeepening formation nevertheless presents challenges for applications that seek to relate overdeepening characteristics to former or present ice sheet parameters, as we have attempted to achieve in our example test of a relationship between overdeepening ER and overriding ice velocity. First, changes in ice sheet flow configuration associated with ice sheet and landscape evolution process that span many glacial cycles means some overdeepenings, perhaps in particular ice sheet sectors, may have formed under conditions unlike those that have prevailed in more recent ice sheet history. Second, changes in ice sheet geometry in response to shorter-term climatic variations will affect ice flow patterns and subglacial hydrological gradients, meaning the precise location of in- and outflow points relevant over the time scale of overdeepening formation can never be precisely known. Third, it has been proposed that spatial patterns of erosion and sedimentation at the glacier bed, which are dictated by the ice-surface gradient, mean overdeepening morphology should maintain equilibrium with ice sheet geometry (e.g., Hooke, 1991; Alley et al., 2003). However, the time scales required for subglacial processes to produce adjustments in overdeepening morphology in response to even slow changes in ice sheet geometry are unknown and this assumption may be invalid.

In light of the complex issues described above and poor knowledge of the geology beneath the present ice sheets, our study has developed methods and criteria that utilise information on present ice sheet flow and geometry and, in particular, that focus our analysis on depressions for which a glaciological origin is most secure. This approach is particularly important for analysis of overdeepening morphology because this requires identification of overdeepening adverse and normal slopes and the exclusion of overdeepenings that do not appear to conform to present ice flow configurations. Further, the latter involves a particular focus on features beneath topographically constrained outlet glacier systems where ice-bed processes and characteristics are most likely to demonstrate equilibria with present ice geometry. The first important consideration therefore is the identification of depression in- and outflow points, for which we utilised ice-surface elevation to infer the points of maximum ice flux into and out of each depression (section 4.1.3). Prediction of in- and outflow points using subglacial water fluxes is unsuitable because flow is sensitive to subtle changes in ice-surface gradient that may cause flow to 'pond' or deviate around the adverse slope. In formerly glaciated terrains, the absence of an overlying ice sheet will mean even greater uncertainty concerning the location of in- and outflow points, especially for depressions in former subglacial mountain ranges or ice sheet interiors.

The second important consideration is overdeepening planform morphology and context because overdeepenings that do not have simple ovoid forms and that are elongate in the direction of ice flow are likely to be nonglacial or 'relict' features. These are therefore unlikely to possess morphologies that are in equilibria with ice sheet processes. Criteria applied here utilised analyses of planform shape, elongation, and ice flow direction to exclude features with circular or complex planform morphologies and with ovoid morphologies that are not elongate in the direction of ice flow. Given that ice flow configurations in Greenland and Antarctica are likely to be stable over many glacial cycles, and given that assumptions concerning overdeepening planform shape are indeed valid, the application of these criteria should provide a very robust means of limiting the mapped data set to overdeepenings that are appropriate for the investigation of overdeepening evolution and ice-erosion feedbacks. Nevertheless, because the majority of ice sheet flow occurs in outlet glacier or ice stream systems that occupy deep troughs that extend far into the ice sheet interiors (e.g., Morlighem et al., 2014), further confidence can be achieved by means of excluding overdeepenings that are not confined by steep topography. For this study, the high relief threshold used to define topographically confined overdeepenings (section 4.3) therefore limits the data set to overdeepenings in deep troughs where ice flow configuration is likely to be highly stable.

6.2. Potential application to overdeepening form

Exploration of the formation and evolution of overdeepenings under contemporary ice sheets offers significant advantages. First, the presence of ice cover means landform morphology in areas of deep erosion is not obscured by post-glacial sedimentation, which complicates analyses of overdeepenings and other erosional features, including tunnel valleys, in palaeo settings (Huuse, 2000; Hansen et al., 2009; Preusser et al., 2010; Moreau and Huuse, 2014). Second, the data that are available that describe ice sheet characteristics, including velocity and thermal regime, are vastly superior to that which can be obtained for former ice sheets, for example from numerical modelling. Third, the present ice sheets have remained largely stable features for much of the recent geological past (e.g., Huybrechts, 1993), meaning landscapes and landforms shaped by characteristically slow subglacial processes, and the ice sheets themselves, are more likely to have achieved equilibrium forms that are in balance with climatic, glaciological, and tectonic forces. Further, the proposed ability of overdeepening form to maintain equilibrium with ice geometry (see section 6.1) means the existence of subglacial sediments within overdeepenings does not necessarily preclude the ability to obtain process insights.

Exploration of the full range of potential applications of our methods is beyond the scope of this paper. Rather, as a single illustration of the potential power of our approach, we have tested for a possible relationship between overdeepening ER and overriding ice velocity. It is nevertheless recognised that

evidence for such a relationship is not at all strong, and this motivates consideration of data and methodological limitations that similar studies must address.

Whilst data set limitations are considered in the section below, methodological limitations concern the validity of the proposal relationship and the ability of the data to provide a robust test. The validity of the relationship is supported by analogy with other glacigenic landforms. Nevertheless, substantial scatter could indicate a variety of confounding factors. First, numerous factors are likely to play a role in overdeepening morphology. For example, it is likely that elongation ratio is influenced by valley width, meaning width is constrained in a way that length is not; whilst it is also possible erosion processes do not necessarily scale linearly with ice velocity (cf. the likely influence on quarrying rates of subglacial water pressure variation; e.g., Hooke, 1991; Egholm et al., 2012). Further consideration also needs to be given to the significance of 'nested' depressions, which may indicate several different processes and controls. Second, the likely time scales of overdeepening formation mean measured ice velocity is not necessarily indicative of mean ice velocity over the time scale of overdeepening formation, and, third, the complexity of subglacial landscapes indicates that filtering methods that attempt to exclude depressions that are unrelated to present ice flow configurations may require refinement. For example, limiting the mapped data set to elongated and topographically confined depressions, which intends to focus analysis on overdeepenings in fast-moving outlet glacier systems that extend inward from the ice sheet margins, will not necessarily exclude overdeepenings in buried mountain ranges in the cold-based interior of the East Antarctic Ice Sheet, which may have formed under warm, early ice sheet conditions (e.g., Bo et al., 2009). Finally, the role of adverse slopes in providing backstress and elevating basal water pressures means overdeepenings may have contrasting implications for ice velocity depending on the specific morphology of the adverse slope.

These limitations and others are likely to be relevant to study of other aspects of overdeepening form, including adverse slope morphology and its significance. Notably, sparse data on subglacial process rates and sediment fluxes mean it is impossible to have confidence that overdeepening morphologies are able to maintain equilibrium with ice sheet processes. For Antarctica in particular, slower rates of subglacial erosion and sediment transport may result in overdeepening morphologies remaining in permanent disequilibrium. In addition, modelling evidence indicates rapid landscape evolution during initial glacial cycles, followed by relative landscape stability (e.g., Kessler et al., 2008; Jamieson et al., 2010), meaning long-lived erosional features that include overdeepenings reflect conditions that prevail early in ice sheet history and are not typical of the present day. Finally, we recognise that different mapping approaches may be required where it is necessary to understand the importance of specific subglacial processes. For example, the subglacial lakes prevalence and morphology reflects

'closed depressions' in the subglacial hydraulic gradient (e.g., Livingstone et al., 2013) that are qualitatively and quantitatively different from their topographic counterparts.

6.3. Data limitations, quality control, and methodological recommendations

The quality of mapping results and the process-based insights that can be obtained using associated empirical data are dependent on the resolution and quality of available bed topography data. In addition, artefacts may be introduced during interpolation of raw bed-elevation measurements. For mapping and analysis of overdeepenings, automated methods can be used to exclude artefact depressions, but these are not without problems.

A major limitation, particularly for Bedmap2, is the absolute uncertainty of large swathes of the subglacial topography. For some areas of the East Antarctic interior, absolute bed-elevation uncertainties range up to 1008 m (Fretwell et al., 2013). Conversely, for the most recent DEM covering Greenland (Bamber et al., 2013), some of the largest errors occur in the mountainous coastal fjord regions where extrapolation, rather than interpolation, has been required to resolve bed elevations. These fjord regions are prime locations for overdeepening development, where topographic confinement dominates the configuration of outflowing ice. Nevertheless, comparison of features mapped from large-scale data sets with those from higher resolution subset domains (e.g., Fig. 9) reveals an encouraging level of consistency. Notably, for the Byrd Glacier depression (Figs. 9C–D), long-profile form (Fig. 9E) is resolved relatively well by Bedmap2 in comparison to the higher-resolution product, with only minor differences in maximum absolute depth. On the other hand, the size, form, and number of smaller depressions in the Byrd Catchment (Figs. 9C-D) is very much influenced by flightline density (Figs. 9A–B), and artefact depressions created at flightline intersections by the interpolation method (i.e., kriging) are evident at both data set resolutions. Quality control criteria that remove such depressions, as applied in the example study above, are therefore necessary regardless of resolution. Acquisition of even higher-resolution data sets using novel extrapolation approaches (e.g., Morlighem et al., 2014) offers the potential to further understand and improve bed-elevation uncertainties, but kriging is still required where ice flow velocities are low and empirical ice thickness measurements are scarce. The scarcity of empirical measurements across large areas of the present ice sheets means therefore that significant areas of uncertainty will remain.

Morphological studies of subglacial phenomena thus require strict appreciation of the uncertainties inherent within the source data sets. The application of multiple quality criteria to mapped results, such as minimum flightline density, is viewed as essential to minimise the introduction of unreliable or spurious data. As such, the limitations of existing subglacial topography data sets mean that the subglacial area that is suitable for landform analyses of the kind presented here is only a fraction of the

total area (e.g., only 36% of the grounded Antarctic bed is constrained by measured data at a 5-km resolution in Bedmap2). Formerly glaciated areas on the adjacent continental shelves offer potential to greatly increase the mappable area: for example, studies in Antarctica show that glacial and post-glacial sedimentation in offshore areas may be only 4-5 m thick (e.g., Dowdeswell et al., 2004) and is therefore well below the minimum bed elevation uncertainty in subglacial areas. However, detailed sediment thickness data for offshore areas is available for only restricted areas, and there is limited potential to relate landform location and morphology to ice sheet parameters. In addition, fjord depths are poorly constrained along much of the Greenland coastline, meaning subglacial and offshore topographies are often mismatched by as much as several hundred metres (Bamber et al., 2013). Further strategic data collection is therefore required to address areas of uncertainty, in the interiors of ice sheets and at present ice-sheet margins.

7. Conclusions

High-resolution bed-topography data sets for the extant ice sheets (Bamber et al., 2013; Fretwell et al., 2013) provide a major opportunity to advance our understanding of subglacial landscape evolution, subglacial processes, and feedbacks between ice sheet and landscape dynamics. Overdeepenings are a key landform in this respect because of the lack of consensus on their origin and their far-reaching influence on critical ice-bed processes and ice sheet behaviour (cf. Cook and Swift, 2012). To address the need for quantitative data on overdeepening characteristics, we have explored automated methods for mapping overdeepenings and the characterisation of overdeepening form. Our main methodological findings can be summarised as follows:

- Hydrological tools and terrain filtering methods fail to adequately capture the complex morphologies of overdeepenings, primarily because terrain filtering lacks precise thresholds required for delimiting closed-depression boundaries and because both methods lack the ability to resolve depression nesting.
- A novel, rule-based GIS method has been proposed that quantitatively tracks changes in the length of closed contours from initial points of elevation minima. This method provides robust mapping results and is computationally efficient at ice sheet scales. Its application is not dependent on a particular bed-data set resolution, requires no abstract threshold parameters to be defined, and is unlikely to be restricted or compromised by anticipated improvements in data set quality and detail.
- The limitations of available data sets mean that mapped features require robust scrutiny. A suite of simple quality control criteria have been proposed that are applicable to the 1-km

gridded data sets for Greenland and Antarctica and are adaptable to different bed topography sources or applications.

We have illustrated our method by testing for a possible relationship between overdeepening elongation ratio and overriding ice velocity using a large sample of depressions mapped beneath the Antarctic and Greenland ice sheets, and we have discussed the potential insights and limitations that are demonstrated by such an approach. We conclude that:

- The ability to relate overdeepening characteristics to present ice sheet characteristics indicates significant potential to gain insight into critical ice-bed processes and feedbacks. However, the limitations of present data sets and the simplicity of our approach mean that strong statistical relationships cannot necessarily be expected.
- Quality criteria are necessary when analysing subglacial topography data sets. Criteria can avoid the inclusion of spurious depressions arising from DEM artefacts and address limitations associated with the density and accuracy of bed-elevation measurements. However, the level of insight that can be acquired is dependent upon the quality of the metrics that such data permit.
- A relationship between overdeepening ER and ice velocity was not ruled out, and given anticipated improvements in data set accuracy and resolution, further work may be warranted. Possible confounding factors, in addition to data set uncertainties, include the existence of additional controls on overdeepening length or width and the long timescale of overdeepening formation relative to that of the climatic changes that influence present ice sheet velocities.
- The significance of reverse bed slopes in glacial systems (Cook and Swift, 2012) indicates that the introduction of overdeepenings into ice sheet beds is itself expected to accelerate or modulate ice velocities, meaning overdeepening characteristics may demonstrate nonlinear relationships with ice velocity.

This work demonstrates that mapping and analysis of even the largest subglacial landforms (including troughs, cirques and overdeepenings) will be an exercise marked with varying aspects of uncertainty that requires strict quality control procedures and close scrutiny of mapping and other outputs. Nevertheless, anticipated improvements in the accuracy and resolution of bed topography data sets, including novel extrapolation methods that utilise surface ice velocities, will reduce the need for quality control procedures and achieve convergence of measured landform attributes on ‘true’ values that will facilitate increasingly robust insights from empirical data. We encourage collaboration between the geomorphological, glaciological, and numerical modelling communities to identify real

and simulated landscape features and IWSE feedbacks that maximise the potential to test simulated landscapes and to expedite process understanding.

Acknowledgements

DAS and HP acknowledge funding from the National Cooperative for the Disposal of Radioactive Waste (NAGRA). CReSIS data used in this study was generated with support from NSF grant ANT-0424589 and NASA Operation IceBridge grant NNX13AD53A. Discussions with Andrew Sole and Jeremy Ely helped to advance ideas produced in this study and their input is gratefully acknowledged. We also acknowledge constructive reviews provided by three anonymous reviewers, which resulted in significant improvements to our manuscript.

References

Alley, R.B., Lawson, D.E., Larson, G.J., Evenson, E.B., Baker, G.S., 2003. Stabilizing feedbacks in glacier-bed erosion. Nature 424, 758–60. doi:10.1038/nature01839

Anderson, R.S., Molnar, P., Kessler, M.A., 2006. Features of glacial valley profiles simply explained. J. Geophys. Res. Earth Surf. 111, F01004.

Arnold, N., 2010. A new approach for dealing with depressions in digital elevation models when calculating flow accumulation values. Prog. Phys. Geogr. 34, 781–809. doi:10.1177/0309133310384542

Bamber, J.L., Griggs, J.A., Hurkmans, R.T.W.L., Dowdeswell, J.A., Gogineni, S.P., Howat, I., Mouginot, J., Paden, J., Palmer, S., Rignot, E., Steinhage, D., 2013. A new bed elevation dataset for Greenland. Cryosph. 7, 499–510. doi:10.5194/tc-7-499-2013

Bo, S., Siegert, M.J., Mudd, S.M., Sugden, D., Fujita, S., Xiangbin, C., Yunyun, J., Xueyuan, T., Yuanshen, L., 2009. The Gamburtsev mountains and the origin and early evolution of the Antarctic Ice Sheet. Nature 459, 690–693.

Boulton, G.S., 1996. Theory of glacial erosion, transport and deposition as a consequence of subglacial sediment deformation J. Glaciol. 42, 43–62.

Brenning, A., 2009. Benchmarking classifiers to optimally integrate terrain analysis and multispectral remote sensing in automatic rock glacier detection. Remote Sens. Environ. 113, 239–247. DOI: 10.1016/j.rse.2008.09.005

Clark, C.D., 1993. Mega-scale glacial lineations and cross-cutting ice-flow landforms. Earth Surf. Process. Landforms 18, 1–29. DOI: 10.1002/esp.3290180102

Clark, C.D., Hughes, A.L.C., Greenwood, S.L., Spagnolo, M., Ng, F.S.L., 2009. Size and shape characteristics of drumlins, derived from a large sample, and associated scaling laws. Quat. Sci. Rev. 28, 677–692. doi:10.1016/j.quascirev.2008.08.035

Clarke, G.K.C., 2005. Subglacial Processes. Annu. Rev. Earth Planet. Sci. 33, 247–276. doi:10.1146/annurev.earth.33.092203.122621

Cook, S.J., Swift, D.A., 2012. Subglacial basins: Their origin and importance in glacial systems and landscapes. Earth-Science Rev. 115, 332–372. DOI: 10.1016/j.earscirev.2012.09.009

Creyts, T.T., Clarke, G.K.C., 2010. Hydraulics of subglacial supercooling: Theory and simulations for clear water flows. J. Geophys. Res. Earth Surf. 115, F03021.

Dowdeswell, J.A., Cofaigh, C.Ó., Pudsey, C.J., 2004. Thickness and extent of the subglacial till layer beneath an Antarctic paleo–ice stream. Geology 32, 13–16. doi:10.1130/G19864.1

Drăguţ, L., Blaschke, T., 2006. Automated classification of landform elements using object-based image analysis. Geomorphology 81, 330–344. DOI: 10.1016/j.geomorph.2006.04.013

Egholm, D., Knudsen, M., Clark, C., 2011. Modeling the flow of glaciers in steep terrains: The integrated second-order shallow ice approximation (iSOSIA). J. Geophys. Res. Earth Surf. 116, F02012.

Egholm, D.L., Pedersen, V.K., Knudsen, M.F., Larsen, N.K., 2012. On the importance of higher order ice dynamics for glacial landscape evolution. Geomorphology 141-142, 67–80. doi:10.1016/j.geomorph.2011.12.020

Esteban, F.D., Tassone, A., Lodolo, A. Menichetti, M., Lippai, H., Waldmann, N., Darbo, A., Baradello, L., Vilas, J. F. 2014. Basement geometry and sediment thickness of Lago Fagnano (Tierra del Fuego). Andean Geol. 41, 293–313.

Evans, I.S., 1980. An integrated system of terrain analysis and slope mapping. Zeitschrift fur Geomorphol. Suppl-Bd 3, 274–295.

Fountain, A.G., Walder, J.S., 1998. Water flow through temperate glaciers. Rev. Geophys. 36, 299–328. doi:10.1029/97RG03579

Fowler, A.C. 2009. Instability modelling of drumlin formation incorporating lee-side cavity growth. Proc. R. Soc. London, Ser. A 465, 2681–2702.

Fowler, A.C. 2010. The instability theory of drumlin formation applied to Newtonian viscous ice of finite depth. Proc. R. Soc. London, Ser. A 466, 2673–2694.

Fowler, A.C., Spagnolo, M., Clark, C.D., Stokes, C.R., Hughes, A.L.C., Dunlop, P., in press. On the size and shape of drumlins. International Journal on Geomathematics.

Fretwell, P., Pritchard, H.D., Vaughan, D.G., Bamber, J.L., Barrand, N.E., Bell, R., Bianchi, C., Bingham, R.G., Blankenship, D.D., Casassa, G., Catania, G., Callens, D., Conway, H., Cook, A.J., Corr, H.F.J., Damaske, D., Damm, V., Ferraccioli, F., Forsberg, R., Fujita, S., Gim, Y., Gogineni, P., Griggs, J.A., Hindmarsh, R.C.A., Holmlund, P., Holt, J.W., Jacobel, R.W., Jenkins, A., Jokat, W., Jordan, T., King, E.C., Kohler, J., Krabill, W., Riger-Kusk, M., Langley, K.A., Leitchenkov, G., Leuschen, C., Luyendyk, B.P., Matsuoka, K., Mouginot, J., Nitsche, F.O., Nogi, Y., Nost, O.A., Popov, S. V., Rignot, E., Rippin, D.M., Rivera, A., Roberts, J., Ross, N., Siegert, M.J., Smith, A.M., Steinhage, D., Studinger, M., Sun, B., Tinto, B.K., Welch, B.C., Wilson, D., Young, D.A., Xiangbin, C., Zirizzotti, A., 2013. Bedmap2: improved ice bed, surface and thickness datasets for Antarctica. Cryosph. 7, 375–393. doi:10.5194/tc-7-375-2013

Glasser, N.F., Bennett, M.R., 2004. Glacial erosional landforms: origins and significance for palaeoglaciology. Prog. Phys. Geogr. 28, 43–75. doi:10.1191/0309133304pp401ra

Hallet, B., Hunter, L., Bogen, J., 1996. Rates of erosion and sediment evacuation by glaciers: A review of field data and their implications. Global Planet. Change 12, 213–235.

Hansen, L., Beylich, A., Burki, V., Eilersten, R.S., Fredin, O., Larsen, E., Lysså, A., Nesje, A., Stalsberg, K., Tønnesen, J.F., 2009. Stratigraphic architecture and infill history of a deglaciated bedrock valley based on georadar, seismic profiling and drilling. Sedimentology 56, 1751–1773. doi:10.1111/j.1365-3091.2009.01056.x

Harbor, J.M., 1992. Numerical modeling of the development of U-shaped valleys by glacial erosion. Geol. Soc. Am. Bull. 104 (10), 1364–1375.

Heidenreich, C., 1964. Some observations on the shape of drumlins. Can. Geogr. 8, 101–107. doi:10.1111/j.1541-0064.1964.tb00591.x

Herman, F., Beaud, F., Champagnac, J.D., Lemieux, J.M., Sternai, P., 2011. Glacial hydrology and erosion patterns: a mechanism for carving glacial valleys. Earth Planet. Sci. Lett. 310, 498–508. DOI: 10.1016/j.epsl.2011.08.022

Hooke, R.L., 1991. Positive feedbacks associated with erosion of glacial cirques and overdeepenings. Geol. Soc. Am. Bull. 103, 1104–1108. doi: 10.1130/0016-7606(1991)103<1104:PFAWEO>2.3.CO;2

Huuse, M., 2000. Overdeepened Quaternary valleys in the eastern Danish North Sea: morphology and origin. Quat. Sci. Rev. 19, 1233–1253. doi:10.1016/S0277-3791(99)00103-1

Huybrechts, P., 1993. Glaciological modelling of the late Cenozoic East Antarctic ice sheet: Stability or dynamism? Geogr. Ann. A 75, 221–238. DOI: 10.2307/521202

Iverson, N. R., 2012. A theory of glacial quarrying for landscape evolution models. Geology 40, 679–682.

Iverson, N.R., Hanson, B., Hooke, R.L., Jansson, P., 1995. Flow mechanism of glaciers on soft beds. Science 267, 80–81.Jakobsson, M., Mayer, L., Coakley, B., Dowdeswell, J.A., Forbes, S., Fridman, B., Hodnesdal, H., Noormets, R., Pedersen, R., Rebesco, M., Schenke, H.W., Zarayskaya, Y., Accettella, D., Armstrong, A., Anderson, R.M., Bienhoff, P., Camerlenghi, A., Church, I., Edwards, M., Gardner, J. V., Hall, J.K., Hell, B., Hestvik, O., Kristoffersen, Y., Marcussen, C., Mohammad, R., Mosher, D., Nghiem, S. V., Pedrosa, M.T., Travaglini, P.G., Weatherall, P., 2012. The International Bathymetric Chart of the Arctic Ocean (IBCAO) Version 3.0. Geophys. Res. Lett. 39, L12609. doi:10.1029/2012GL052219

Jamieson, S.S.R., Sugden, D.E., Hulton, N.R.J., 2010. The evolution of the subglacial landscape of Antarctica. Earth Planet. Sci. Lett. 293, 1–27. doi:10.1016/j.epsl.2010.02.012

Joughin, I.B., Smith, B., Howat, I., Scambos, T.A., 2010a. MEaSUREs Greenland Ice Sheet Velocity Map from InSAR Data. National Snow and Ice Data Center., Boulder, Colorado USA. doi:nsidc-0478.001

Joughin, I.B., Smith, B.E., Howat, I.M., Scambos, T., Moon, T., 2010b. Greenland flow variability from ice-sheet-wide velocity mapping. J. Glaciol. 56, 415–430. doi:10.3189/002214310792447734

Kessler, M.A., Anderson, R.S., Briner, J.P., 2008. Fjord insertion into continental margins driven by topographic steering of ice. Nat. Geosci. 1, 365–369. doi:10.1038/ngeo201

King, E.C., Hindmarsh, R.C.A., Stokes, C.R., 2009. Formation of mega-scale glacial lineations observed beneath a West Antarctic ice stream. Nat. Geosci. 2, 585–588. doi:10.1038/ngeo581

Klingseisen, B., Metternicht, G., Paulus, G., 2008. Geomorphometric landscape analysis using a semi-automated GIS-approach. Environ. Model. Softw. 23, 109–121. DOI: 10.1016/j.envsoft.2007.05.007

Leonowicz, A.M., Jenny, B., Hurni, L., 2009. Automatic generation of hypsometric layers for small-scale maps. Comput. Geosci. 35, 2074–2083. doi:10.1016/j.cageo.2008.12.012

Livingstone, S.J., Clark, C.D., Woodward, J., Kingslake, J., 2013. Predicting subglacial lakes and meltwater drainage pathways beneath the Antarctic and Greenland ice sheets. The Cryosphere 7, 1721–1740.

MacGregor, K.R., Anderson, R.S., Anderson, S.P., Waddington, E.D., 2000. Numerical simulations of glacial-valley longitudinal profile evolution. Geology 28, 1031–1034.

MacMillan, R.A., Pettapiece, W.W., Nolan, S.C., Goddard, T.W., 2000. A generic procedure for automatically segmenting landforms into landform elements using DEMs, heuristic rules and fuzzy logic. Fuzzy Sets Syst. 113, 81–109. DOI: 10.1016/S0165-0114(99)00014-7

Moreau, J., Huuse, M., 2014. Infill of tunnel valleys associated with landward-flowing ice sheets: The missing Middle Pleistocene record of the NW European rivers? Geochemistry, Geophys. Geosystems 15, 1–9. doi:10.1002/2013GC005007

Morlighem, M., Rignot, E., Mouginot, J., Seroussi, H., Larour, E., 2014. Deeply incised submarine glacial valleys beneath the Greenland ice sheet. Nat. Geosci. 7, 418–422. doi:10.1038/ngeo2167

Nick, F.M., Vieli, A., Howat, I.M., Joughin, I., 2009. Large-scale changes in Greenland outlet glacier dynamics triggered at the terminus. Nat. Geosci. 2, 110–114. doi:10.1038/ngeo394

Ó Cofaigh, C., Stokes, C.R., Lian, O.B., Clark, C.D., Tulacyzk, S., 2013. Formation of mega-scale glacial lineations on the Dubawnt Lake Ice Stream bed: 2. Sedimentology and stratigraphy. Quat. Sci. Rev. 77, 210–227. doi:10.1016/j.quascirev.2013.06.028

Patton, H., Swift, D.A., Clark, C.D., Livingstone, S., Cook, S.J., in prep. Distribution and characteristics of overdeepenings beneath the Greenland and Antarctic ice sheets. Quat. Sci. Rev.

Preusser, F., Reitner, J.M., Schlüchter, C., 2010. Distribution, geometry, age and origin of overdeepened valleys and basins in the Alps and their foreland. Swiss J. Geosci. 103, 407–426. doi:10.1007/s00015-010-0044-y

Rignot, E., Mouginot, J., Scheuchl, B., 2011a. MEaSUREs InSAR-Based Antarctica Ice Velocity Map. National Snow and Ice Data Center, Boulder, Colorado USA. doi:nsidc-0484.001

Rignot, E., Mouginot, J., Scheuchl, B., 2011b. Ice flow of the Antarctic ice sheet. Science (80-.). 333, 1427–30. doi:10.1126/science.1208336

Roberts, D.H., Long, A.J., Davies, B.J., Simpson, M.J.R., Schnabel, C., 2010. Ice stream influence on West Greenland Ice Sheet dynamics during the Last Glacial Maximum. J. Quat. Sci. 25, 850–864. doi:10.1002/jqs.1354

Ross, N., Siegert, M.J., Woodward, J., Smith, A.M., Corr, H.F.J., Bentley, M.J., Hindmarsh, R.C.A., King, E.C., Rivera, A., 2011. Holocene stability of the Amundsen-Weddell ice divide, West Antarctica. Geology 39, 935–938.

Röthlisberger, H., Lang, H., 1987. Glacial hydrology. In: Gurnell, A.M., Clark, M.J. (Eds.), Glacio-fluvial sediment transfer: an alpine perspective. John Wiley, Chichester.

Saha, K., Wells, N.A., Munro-Stasiuk, M., 2011. An object-oriented approach to automated landform mapping: A case study of drumlins. Comput. Geosci. 37, 1324–1336. DOI: 10.1016/j.cageo.2011.04.001

Schoof, C. 2005.The effect of cavitation on glacier sliding. Proc. R. Soc. A , 461, 609–627.

Schoof, C., 2007. Ice sheet grounding line dynamics: Steady states, stability, and hysteresis. J. Geophys. Res. 112, F03S28. DOI: 10.1029/2006JF000664

Shreve, R.L., 1972. Movement of water in glaciers. J. Glaciol. 11, 205–214.

Stokes, C.R., Clark, C.D., 1999. Geomorphological criteria for identifying Pleistocene ice streams. Ann. Glaciol. 28, 67–74. doi:10.3189/172756499781821625

Stokes, C.R., Clark, C.D., 2002. Are long subglacial bedforms indicative of fast ice flow? Boreas 31, 239–249. doi:10.1111/j.1502-3885.2002.tb01070.x

Stumpf, A., Niethhammer, U., Rothmund, S., Mathieu, A., Malet, J.P., Kerle, N., Joswig, M., 2013. Advanced image analysis for automated mapping of landslide surface fissures, in: Margottini, C., Canuti, P., Sassa, K. (Eds.), Landslide Science and Practice Volume 2: Early Warning, Instrumentation and Monitoring. Springer Berlin Heidelberg, Berlin, Heidelberg, pp. 357–363. doi:10.1007/978-3-642-31445-2

Timmermann, R., Le Brocq, A., Deen, T., Domack, E., Dutrieux, P., Galton-Fenzi, B., Hellmer, H., Humbert, A., Jansen, D., Jenkins, A., Lambrecht, A., Makinson, K., Niederjasper, F., Nitsche, F., Nøst, O.A., Smedsrud, L.H., Smith, W.H.F., 2010. A consistent data set of Antarctic ice sheet

topography, cavity geometry, and global bathymetry. Earth Syst. Sci. Data 2, 261–273. doi:10.5194/essd-2-261-2010

van Rensbergen, P., de Batist, M., Beck, C., Chapron, E., 1999. High-resolution seismic stratigraphy of glacial to interglacial fill of a deep glacigenic lake: Lake Le Bourget, Northwestern Alps, France. Sediment. Geol. 128, 99–129. doi:10.1016/S0037-0738(99)00064-0

Vaughan, D.G., Corr, H.F.J., Ferraccioli, F., Frearson, N., O'Hare, A., Mach, D., Holt, J.W., Blankenship, D.D., Morse, D.L., Young, D.A., 2006. New boundary conditions for the West Antarctic ice sheet: Subglacial topography beneath Pine Island Glacier. Geophys. Res. Lett. 33, L09501. doi:10.1029/2005GL025588

Werder, M.A., Hewitt, I.J., Schoof, C.G., Flowers, G.E., 2013. Modeling channelized and distributed subglacial drainage in two dimensions. J. Geophys. Res. Earth Surf. 118, 1–19.

Wilson, J.P., Gallant, J.C., 2000. Terrain Analysis, Principles and Applications. John Wiley and Sons, Chichester.

Wood, J., 1996. The geomorphological characterisation of digital elevation models. PhD thesis, University of Leicester. http://www.soi.city.ac.uk/~jwo/phd

Figure 1

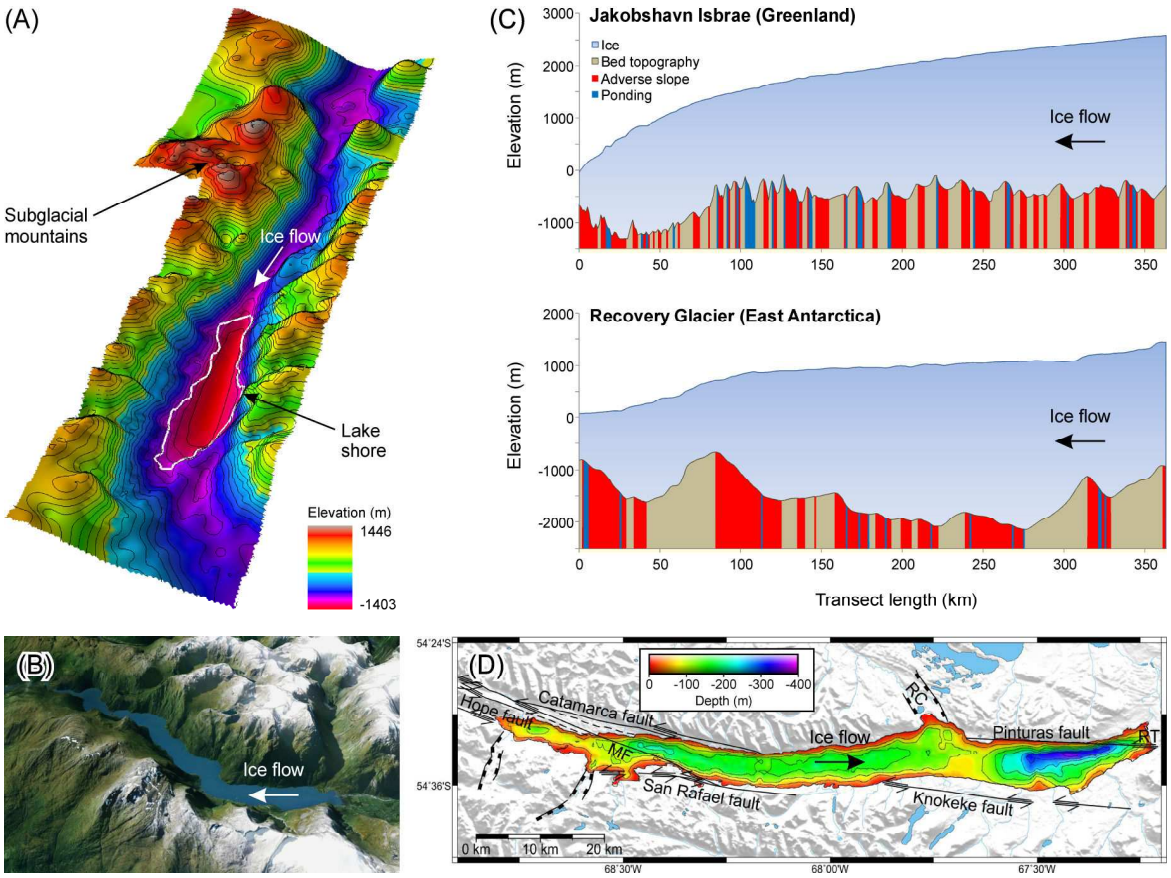

Figure 1. Examples of overdeepenings beneath contemporary and palaeo-ice sheets. (A) Subglacial Lake Ellsworth in East Antarctica (Ross et al., 2011) occupies an overdeepening in a major subglacial trough that cross-cuts the Ellsworth subglacial mountains (figure courtesy Neil Ross). (B) The post-glacial lake Veitastrondvatnet, shown in an oblique aerial view looking due SW, occupies an overdeepening in a sinuous trough confined by the steep topography of the Sognefjord region, Norway. The lake is ~ 17 km long (image: Google Earth). (C) Trough-floor profiles for Jakobshavn Isbrae, Greenland, and Recovery Glacier, Antarctica, derived from bed topography data sets (Bamber et al., 2013; Fretwell et al., 2013), exhibit numerous overdeepenings. Red highlights reverse-bed slopes; blue indicates slope gradients that exceed the ponding threshold (see text). (D) Bathymetry of the bedrock basin occupied by post-glacial Lago Fagnano, Tierra del Fuego, derived from high-resolution, single-channel seismic data, showing numerous 'child' basins in black nested within the 'parent' overdeepening (here defined by the present lake margin). Glacial erosion has been conditioned by tectonic processes and the location of numerous faults. MF: Martínez fault; RT: Río Turbio fault; RC: Río Claro fault. Figure modified from Esteban et al. (2014) .

Figure 2

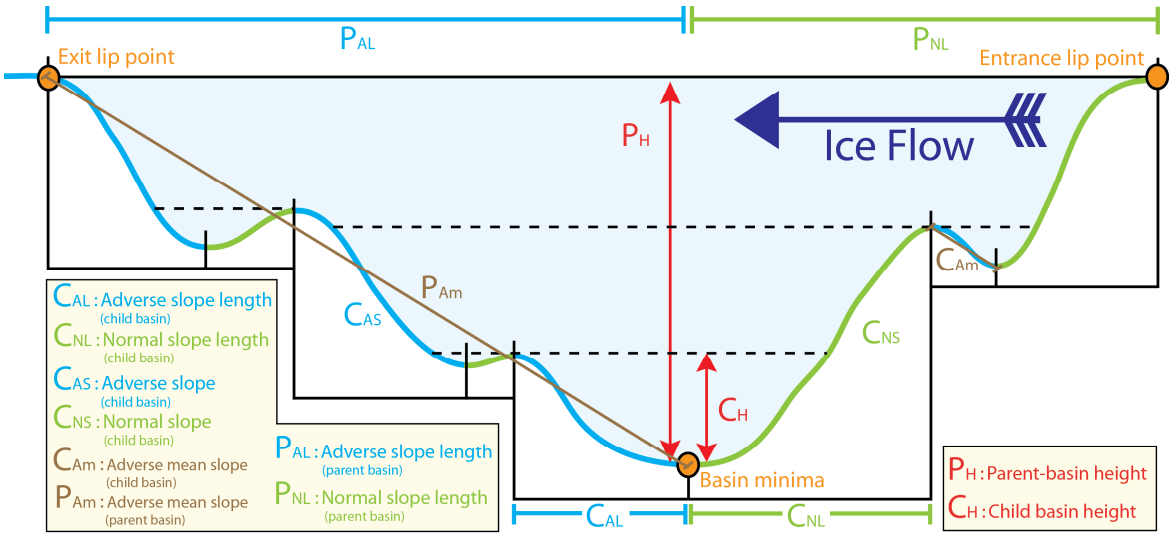

Figure 2. Cartoon showing the long-profile of a subglacial 'parent' depression containing nested 'child' depressions. Various metrics that can be used to describe the form of the depression and associated child depressions are defined.

Figure 3

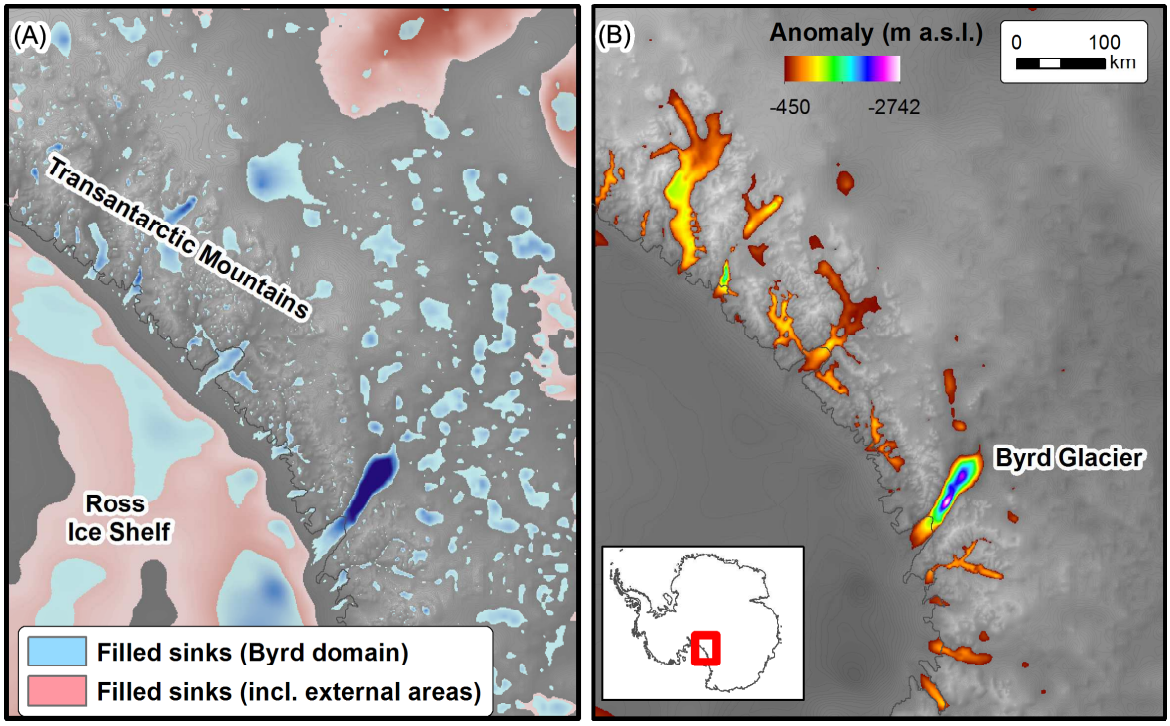

Figure 3. Potential methods for identifying areas of overdeepening, applied to the Bedmap2 DEM. (A) Enclosed depressions mapped using hydrological filling of sinks. Some filled sinks are child depressions (cf. Fig. 2) that are mapped when the method is applied to a small area of the DEM but are not recognised as distinct features when the method is applied across the ice sheet domain. (B) Identification of areas of overdeepening using a low-pass, circular (200 km) Gaussian filter and a standard deviation value of 25. Negative residuals (original elevation values minus filtered elevation values) $\leq$ -450 m are draped over the Bedmap2 topography. Individual overdeepenings and their nestings cannot be discerned.

Figure 4

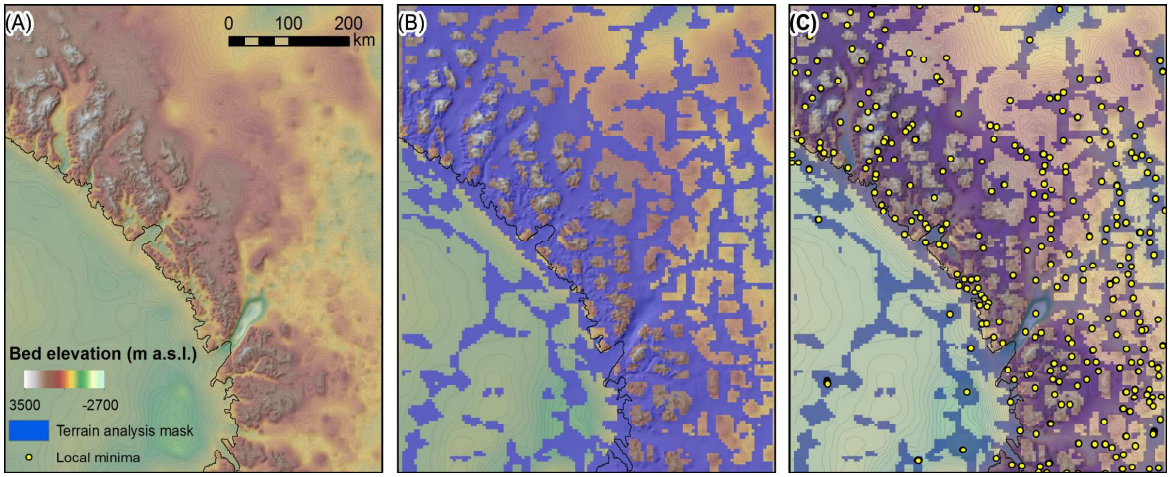

Figure 4. Identification of elevation minima. (A) Initial Bedmap2 DEM; (B) quantitative terrain analysis mask identifying areas of depression-like topography (see text); and (C) points of elevation minima within enclosed depressions (closed contours) contained by the terrain analysis mask.

Figure 5

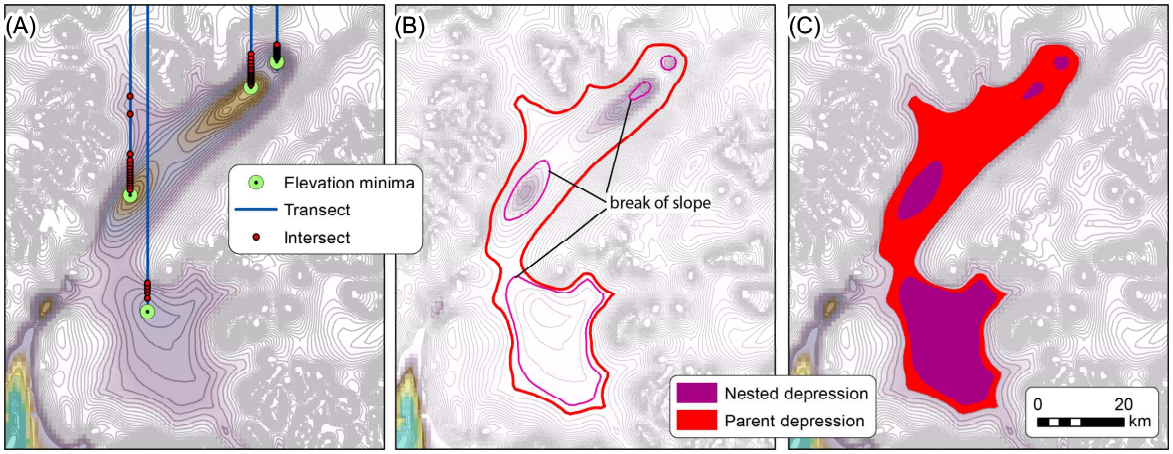

Figure 5. Identification of closed-depression perimeters and their nestings using the contour tracking method. (A) Linear transects drawn from each elevation minima intersect with contours. The length change between adjacent contours is calculated to identify abrupt increases in contour length that indicate that a contour is beyond the contour that defines the closed-depression perimeter (see text). (B) Parent and child depressions are identified using multiple passes of the contour-tracking algorithm and using a threshold contour-length increase of > 90%, corresponding to a break of slope associated with the depression boundary. (C) Parent and child depressions classified using a top-down approach.

Figure 6

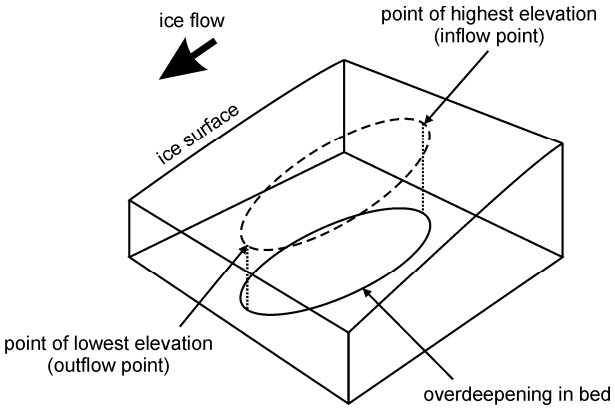

Figure 6. Cartoon illustrating the use of the ice-surface elevation data to identify overdeepening in- and outflow points for an elongate overdeepening oriented in the direction of ice flow. Topographic focussing of ice flow into the overdeepening means these points are suitable proxies for the principal overdeepening entry and exit points in terms of the greatest ice flux.

Figure 7

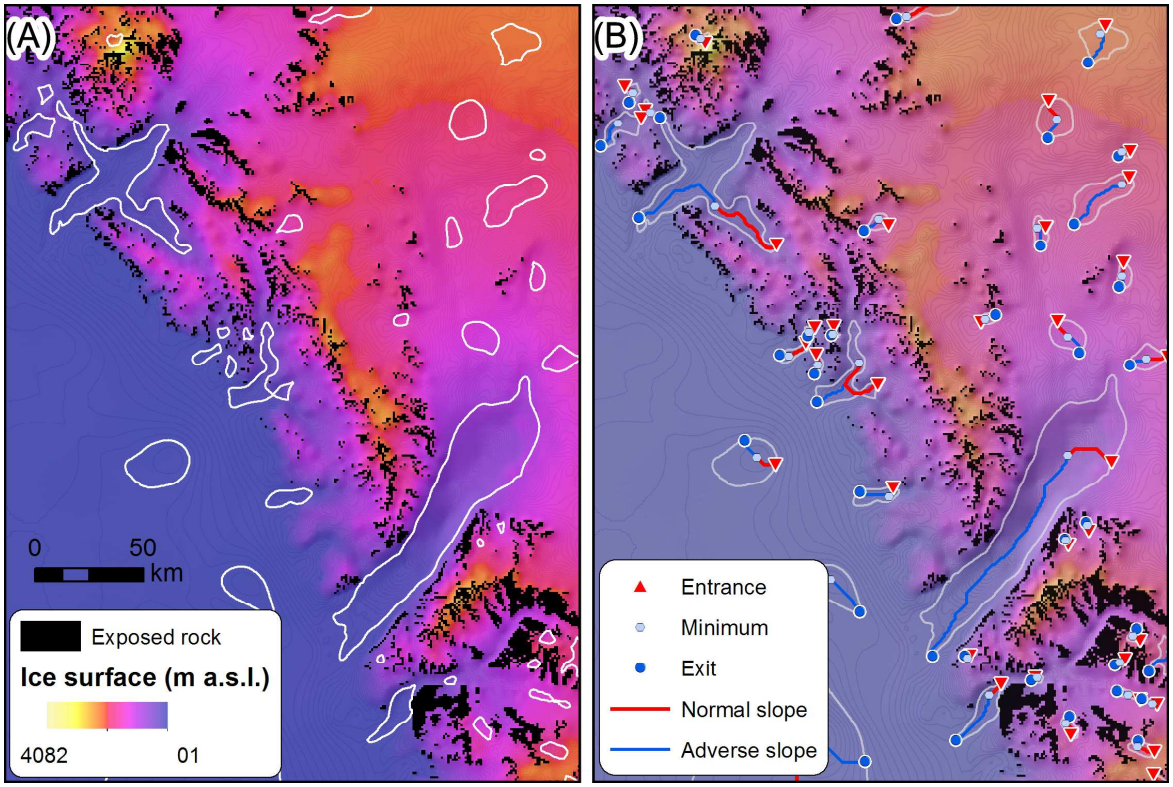

Figure 7. Identification of overdeepening in- and outflow points using ice surface elevation data (cf. Fig. 7) and overdeepening long-profiles. (A) Ice-surface elevation (coloured scale) draped over the Bedmap2 subglacial topography (shading beneath the colour). (B) In- and outflow points of parent depressions identified from (A) and long-profiles, comprising adverse and normal slopes, calculated using a 'least-cost' routing analysis (see text).

Figure 8

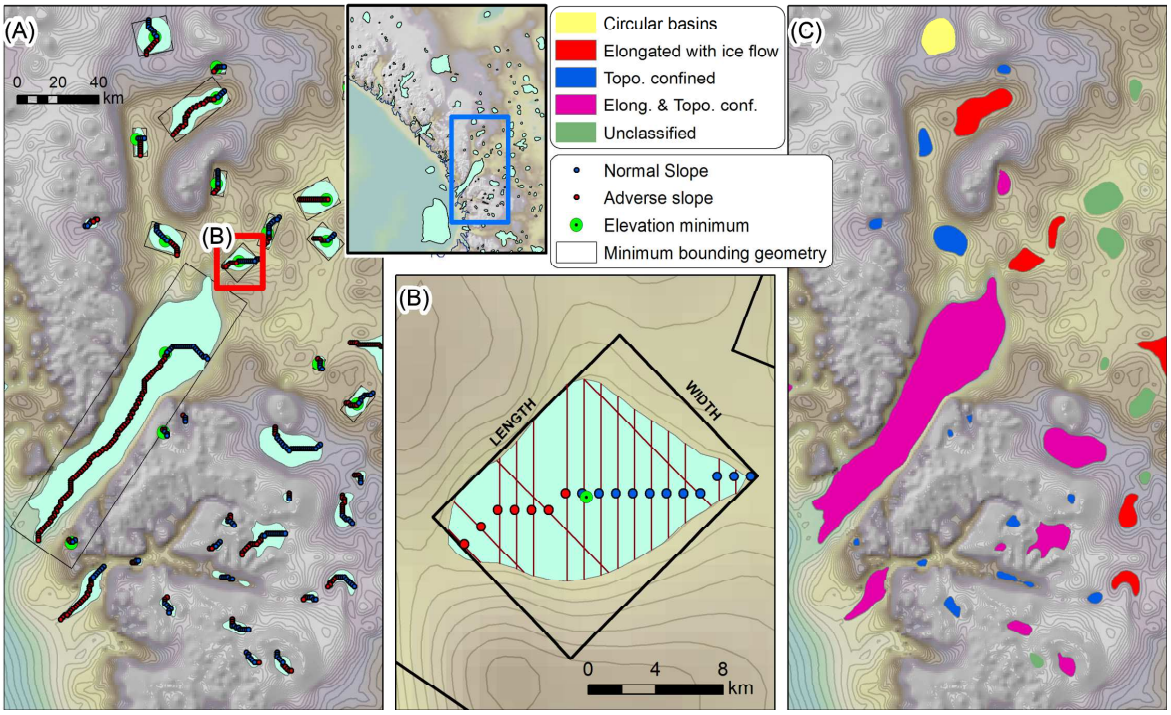

Figure 8. Depression-shape classification methods and results. (A) Parent depressions enclosed by a polygon representing the smallest rectangle possible by area. (B) A magnified view of the depression boxed in red in (A) showing the bounding rectangle and transects (red lines oriented perpendicular to the least-cost path) used to calculate depression mean width. (C) Example classification output.

Figure 9

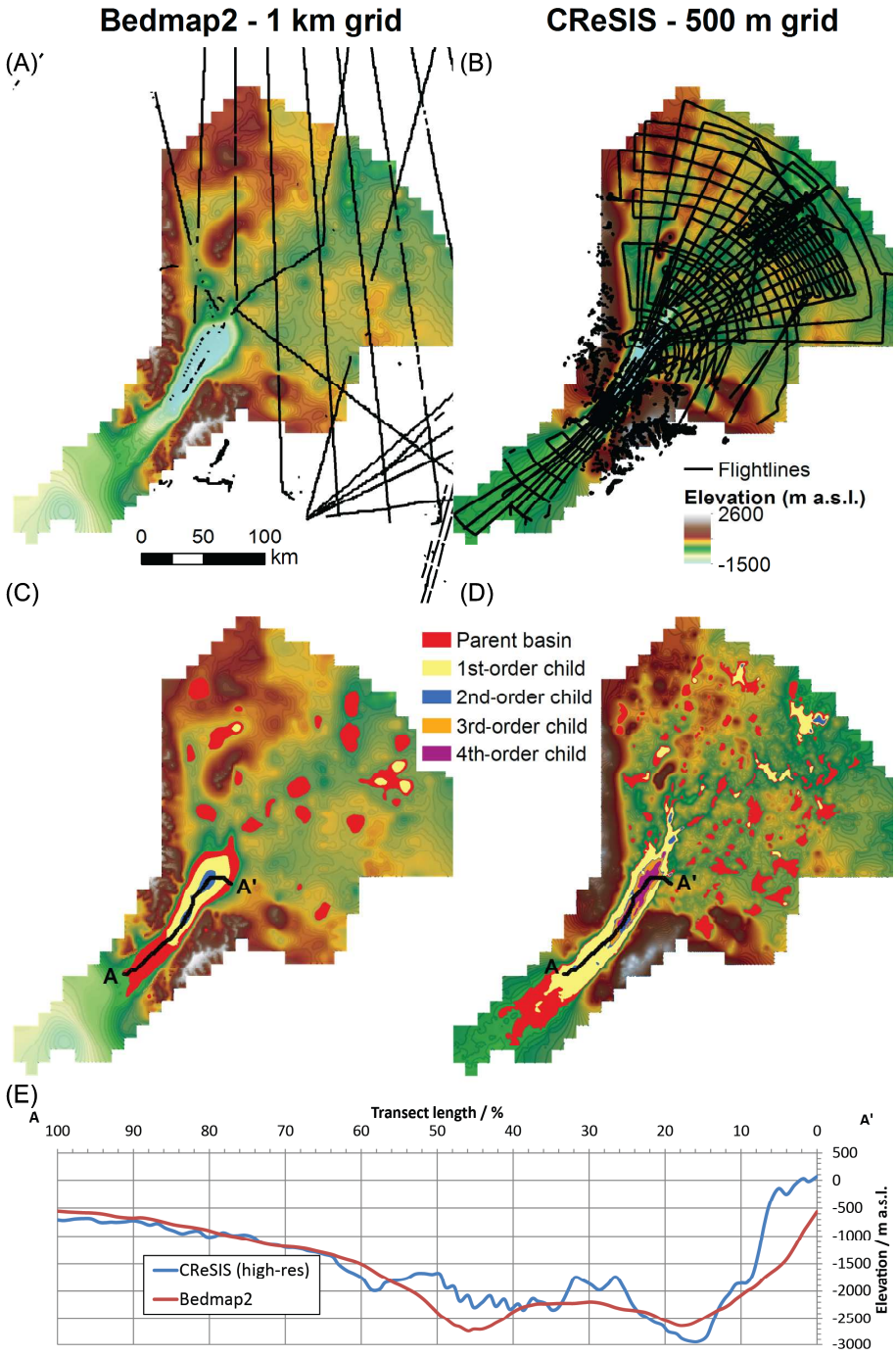

Figure 9. Comparison of subglacial topography, flightline density, and mapping outputs for Bedmap2 versus a higher resolution dataset (CReSIS; see text) covering a sector of the Byrd Glacier catchment. (A–B) Radar flightline tracks (black) and interpolated subglacial topography (see legend in B). (C–D) Mapping results, showing differences in the shape, size and number of parent and child depressions as a consequence of interpolation of data from contrasting flightline densities to produce data sets with contrasting resolutions. (E) Long-profiles for transect A–A' in (C) and (D).

Figure 10

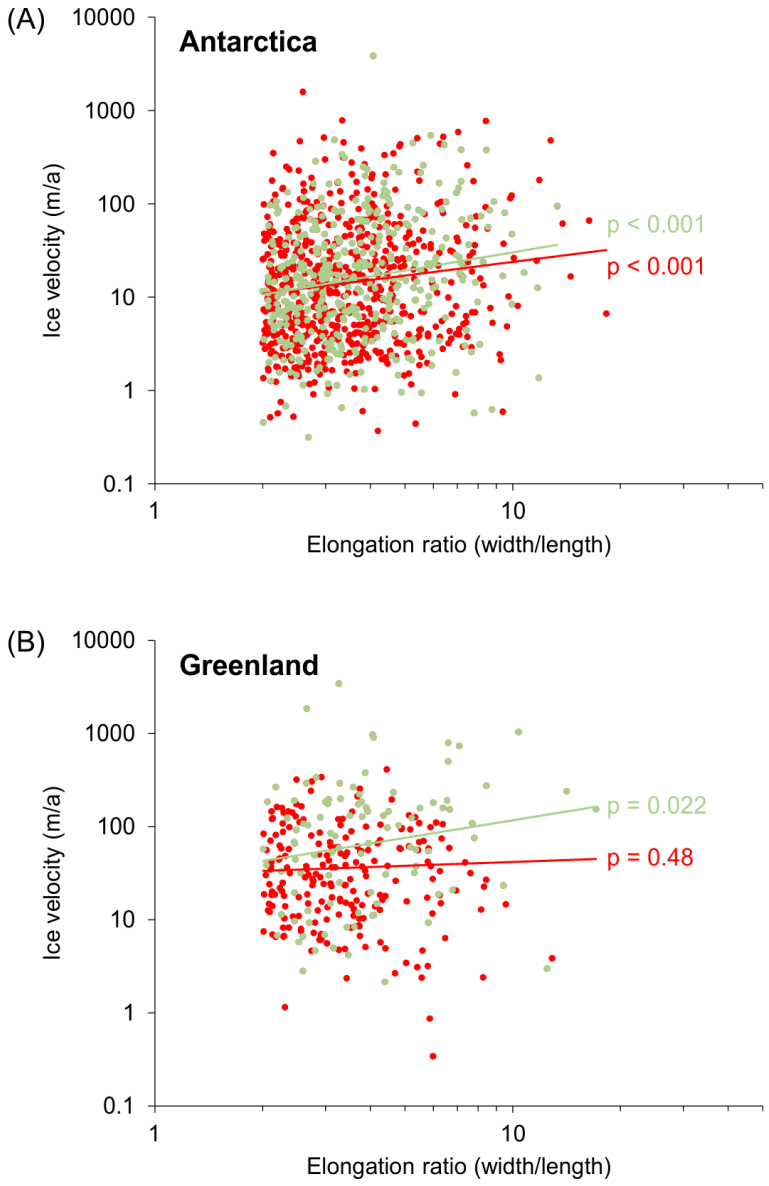

Figure 10. Example application of data on overdeepening form, showing overdeepening elongation ratio versus ice-surface velocity above the overdeepening minima for (A) Antarctica and (B) Greenland. Red points are overdeepenings that are elongated in the direction of ice flow; green points are the subset of these overdeepenings that have been classified as topographically confined. Values for best-fit regression lines show the significance (p) of the regression relationship; R^2 values are ≤ 0.03, reflecting considerable scatter that is discussed in the text.

Table 1

Parameters used in steps 1 to 3 of the contour tracking approach

Parameter	Description/purpose	Value (units)
Step 1: (Terrain analysis mask)		
Plan curvature	Horizontal curvature, intersecting with the XY plane.	>0.00003; <0.001
Minimum curvature	In direction perpendicular to the direction of maximum curvature (which can be any direction).	$< -0.6 \times 10^{-6}$
Mask resolution	Typically up to a magnitude coarser than the DEM resolution.	5000 (m)
Step 2: (Finding elevation minima)		
Contour interval	Elevation distance between contours. Decreasing this value will add computational time needed to find depression lips. Therefore, consideration of the grid resolution should be made when choosing this value.	50 (m)
Step 3: (Contour analysis)		
Maximum perimeter	Set to exclude very large (probably tectonic/plateau) basins.	2×10^{6} (m)
Minimum perimeter	Set to exclude very small depressions that may be artefacts created by interpolation algorithms used in the creation of the DEM.	6×10^{3} (m)
Maximum transect	The length of the transect used for tracking changes in contour length can be set to exclude very large depressions (e.g. tectonic basins, basin-shaped plateaus).	1×10^{5} (m)
Contour-length change	Percentage increase threshold that defines a break of slope, i.e. the depression lip.	190 (%)

Table 2

Merits of alternative methods for the identification of in- and outflow points of individual closed depressions; methods are listed in order of preference

Method	**Description**	**Advantage**	**Disadvantage**
Ice-surface based	Minimum and maximum elevations of the ice-sheet surface at the basin edge are used to indicate probable pour points.	* Most reliable indicator of up/down-ice flow, based from relatively easily accessible measurements taken from the ice surface. * Computationally simple.	* Methodology collapses for basins under relatively flat ice shelves, offshore regions where no ice exists, or where basins may have formed under alternative ice-sheet configurations. * Shallow ice-surface relief can produce multiple possible pour points, making discrimination tricky. * Requires full coverage of an additional empirical dataset, leaving it unsuitable for palaeo domains.
Topography based	Mean elevation across a large (>500-km) moving window is used to calculate the likely direction of ice flow across the domain. Further parameters, including the range of elevation around the basin edge and maximum distance from the basin elevation minima, are used to isolate a single pour point.	* Simple technique requiring no additional datasets.	* Local mountain ranges can affect the correct orientation of up- and down-glacier points, depending on the size of the moving window given.
Hydrology based	Flow accumulation calculations and subaerial network analyses are used to create a stream network across the domain. Pour points are defined from quantifying the magnitude of flow entering and leaving the basin.	* Most reliable for analysing overdeepenings at the valley-scale glaciation. * Useful for highlighting inherited landforms from time-periods of ice-sheet inception.	* Heavily affected by local watersheds; not suitable for analyses at the ice-sheet scale. * Water flow does not necessarily reflect probable ice-flow.